

# Nitric Oxide Binding to the Cardiolipin Complex of Ferric Cytochrome *c*

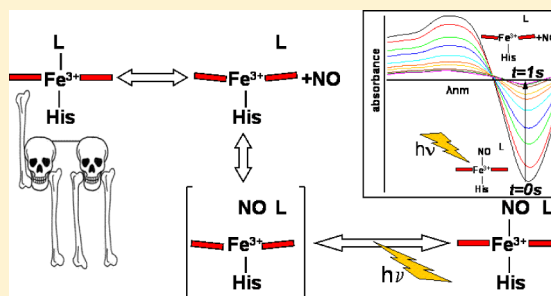
G. Silkstone,<sup>\*,†</sup> S. M. Kapetanaki,<sup>‡</sup> I. Husu,<sup>†</sup> M. H. Vos,<sup>‡</sup> and M. T. Wilson<sup>†</sup>

<sup>†</sup>School of Biological Sciences, University of Essex, Wivenhoe Park, Colchester, C04 3SQ, U.K.

<sup>‡</sup>Laboratoire d'Optique et Biosciences, CNRS Ecole Polytechnique, 91128 Palaiseau, France, and INSERM U696, 91128 Palaiseau, France

**ABSTRACT:** Cardiolipin, a phospholipid specific to the mitochondrion, interacts with the small electron transfer heme protein cytochrome *c* through both electrostatic and hydrophobic interactions. Once in a complex with cardiolipin, cytochrome *c* has been shown to undergo a conformational change that leads to the rupture of the bond between the heme iron and the intrinsic sulfur ligand of a methionine residue and to enhance the peroxidatic properties of the protein considered important to its apoptotic activity. Here we report that the ferric cytochrome *c*/cardiolipin complex binds nitric oxide tightly through a multistep process in which the first step is the relatively slow displacement ( $5\text{ s}^{-1}$ ) from heme coordination of an intrinsic ligand that

replaces methionine in the complex. Nanosecond photolysis of the nitrosyl adduct demonstrated that a fraction of the nitric oxide escapes from the heme pocket and subsequently recombines to the heme in second-order processes ( $k = 1.8 \times 10^6$  and  $5.5 \times 10^5\text{ M}^{-1}\text{ s}^{-1}$ ) that, under these conditions, were much faster than recombination of the intrinsic ligand with which they compete. Ultrafast (femtosecond) laser photolysis showed that the geminate recombination of nitric oxide to the heme occurred with time constants ( $\tau = 22$  and  $72\text{ ps}$ ) and that  $\sim 23\%$  of the photolyzed nitric oxide escaped into the bulk phase. This high value for the escape fraction relative to other heme proteins indicates the open nature of the heme pocket in this complex. These results are summarized in a scheme and are discussed in terms of the possible modulation of the apoptotic activity of cytochrome *c* by nitric oxide.



Cytochrome *c* (cyt *c*) is a small heme-containing redox protein located in the mitochondrial intermembrane space that transfers electrons between the  $bc_1$  complex and the terminal acceptor, cytochrome *c* oxidase. Besides its redox properties, cyt *c* is also involved in apoptosis, programmed cell death. Cardiolipin (CL) is a phospholipid that is specific to mitochondria and plays a critical role in the latter function of cyt *c*.<sup>1</sup> One suggestion for the mechanism of cyt *c*-induced apoptosis is that a fraction of the molecules of cyt *c* is anchored to the outer surface of the mitochondrial inner membrane by electrostatic and hydrophobic interactions with CL. These interactions lead to a change in the tertiary structure of cyt *c*, rendering the heme crevice more open and making the protein display a peroxidase activity that results in the oxidation of CL and subsequently permeabilization of the outer mitochondrial membrane and cyt *c* release.<sup>2,3</sup>

The execution phase of apoptosis is highly regulated at several levels even after the release of cyt *c*,<sup>4,5</sup> and the redox state of cyt *c* has been suggested to play a role.<sup>6,7</sup> The signaling molecules NO and CO are also known to influence apoptosis.<sup>8,9</sup> Our recent work has demonstrated that cyt *c*, reduced in the presence of CL, can bind CO with high affinity and has pointed toward a possible regulatory role for CO.<sup>10</sup> CL was shown to induce significant conformational changes in cyt *c* resulting in heme pocket reorganization coupled with dissociation of the intrinsic methionine ligand.<sup>10</sup> Our studies

of the interaction of the reduced cyt *c*/CL complex with NO have revealed the unexpected binding of NO at the proximal site of cyt *c* in a manner similar to that of cytochrome *c'* and possibly to guanylate cyclase.<sup>11</sup> This unusual mode of binding, specific to NO, also offers a distinct mechanism for NO dissociation and suggests that CL may contribute to a controlled NO release in mitochondria during the early stages of apoptosis that may interfere with the peroxidatic activity of the protein.<sup>12</sup>

These earlier studies focused on the interaction of CO and NO with the reduced form of the cyt *c*/CL complex. In this work, we examine the interaction of NO with the oxidized cyt *c*/CL complex, in an effort to understand the potential role of the oxidation state of cyt *c* in the early stages of apoptosis. NO, unlike CO, is a versatile ligand able to bind to both heme-iron(III) and -iron(II) states giving rise to six-coordinate and five-coordinate heme adducts, respectively.<sup>11,13,14</sup> Study of the NO dynamics can provide significant information about the heme environment, because they are closely related to the protein function and subtly controlled by the protein structure.<sup>15</sup> Therefore, we investigated the fast and ultrafast

Received: May 4, 2012

Revised: July 11, 2012

Published: July 17, 2012





NO dynamics of the oxidized cyt *c*/CL complex to gain insight into the mechanism of NO binding and further appreciation of the role of NO in cyt *c*/CL complex-mediated apoptosis. Our data reveal a significant escape of the bound NO ligand from the heme in the presence of CL, pointing toward the presence of a similarly efficient ligand exchange channel as revealed by our previous studies of the CO and NO dynamics of the reduced cyt *c*/CL complex. The physiological implications of the formation of an oxidized cyt *c*/CL–NO complex are discussed.

## MATERIALS AND METHODS

**Sample Preparation.** Cyt *c* (horse heart) was purchased from Aldrich or Sigma (type IV) and used without further purification. To obtain the ferric NO-bound form of the cyt *c*/CL complex, cyt *c* was dissolved to the desired concentration in 20 mM MOPS (pH 6.7) or 20 mM Hepes (pH 7.4) in a gastight container that was purged with nitrogen to remove oxygen. CL was dissolved in ethanol and added to the cyt *c* solution in an ~25-fold excess. The final concentration of ethanol in solution was generally kept to a maximum of 2% (unless otherwise stated) to avoid polymerization of cyt *c*.<sup>16</sup> The degassed cyt *c*/CL complex was mixed with an NO donor (ProliNONOate, Cayman Chemical Co.) or, for the ultrafast experiments, equilibrated with 0.1 atm of NO. The formation of the complex was verified by UV–vis spectroscopy.

**Static Spectroscopy.** Static absorption spectra were recorded using either a Shimadzu UV–vis 1601 or a Varian Cary SE spectrophotometer.

**Kinetic Measurements.** Stopped-flow spectroscopy was conducted using an Applied Photophysics SX-20 instrument equipped with a diode array accessory. Nanosecond laser flash photolysis measurements were taken using an Applied Photophysics SX-18MV instrument. Data analysis was performed using ProK (Applied Photophysics). Multicolor femtosecond absorption spectroscopy<sup>17</sup> was performed with a 60 fs pulse centered at 560 nm and a white light continuum probe pulse used in the 380–480 nm region, at a repetition rate of 30 Hz. Full spectra of the test and reference beams were recorded using a combination of a polychromator and a CCD camera. Multiple time window acquisition schemes were used, with windows ranging from 4 ps to 4 ns full scale. All experiments were conducted at room temperature. The sample was continuously moved perpendicular to the beams to ensure sample renewal between subsequent pulse pairs. Absorption spectra of all samples were taken before and after the time-resolved measurements to monitor sample stability. The transient absorption data matrix  $\Delta A(\lambda, t)$  was fit to the sum of exponentially decaying components  $\text{DAS}_i e^{-k_i t}$ , in which the  $\text{DAS}_i$  are the decay-associated spectra. The fit procedure is based on singular-value decomposition and has been outlined previously.<sup>18</sup>

## RESULTS

**Static Absorption Spectra.** The static absorption spectra of ferric cyt *c*, the ferric cyt *c*/CL complex, and the NO adduct of this complex at pH 7.4 are shown in Figure 1A. The NO–ferric cyt *c*/CL complex has absorption bands at 415, 528, and 561 nm, which are characteristic for NO-bound heme proteins with histidine as the axial ligand<sup>19</sup> and are consistent with previous studies<sup>20</sup> and with the NO spectrum of cyt *c* in the absence of CL.<sup>21</sup> The spectrum of the ferric cyt *c*/CL complex

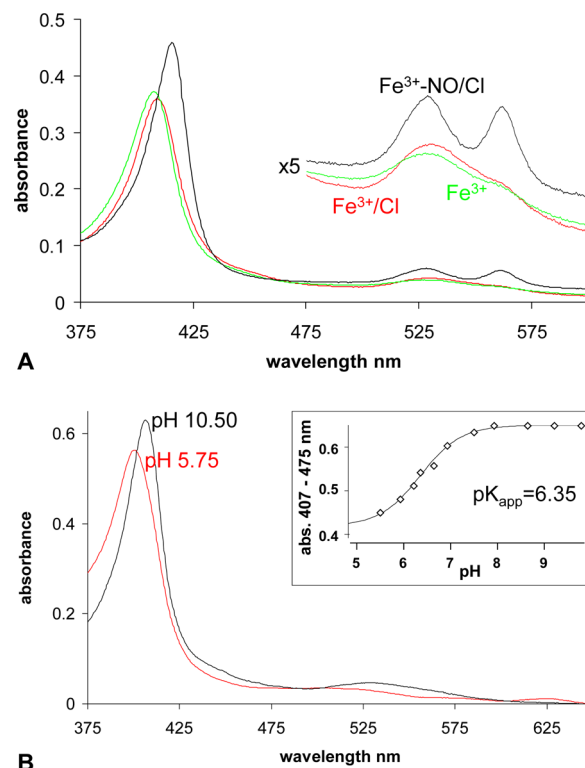


**Figure 1.** (A) Static spectra of the ferric forms of horse heart cyt *c*. Spectrum of the ferric form (green line), the ferric/CL complex (red line), with CL in 25-fold excess over cyt *c*, and the NO adduct of the ferric/CL complex (black line). The amplitudes of the spectra in the visible region are also shown expanded (5-fold). Conditions: ~3  $\mu\text{M}$  cyt *c*, 20 mM Hepes (pH 7.4), 22 °C. (B) pH titration of the ferric cyt *c*/CL complex. The static spectra, the low-pH (5.75) red line and high-pH (10.50) black line, of the ferric cyt *c*/CL complex are shown. The inset shows the pH dependence of the spectrum of the ferric cyt *c*/CL complex. The data were fit using the Henderson–Hasselbalch equation ( $n = 1$ ;  $\text{pK} = 6.35 \pm 0.15$ ). Conditions: ~5  $\mu\text{M}$  cyt *c*, 5 mM sodium acetate, Hepes, and CAPS, 22 °C.

was found to be pH-dependent. The inset of Figure 1B illustrates this showing the complex titrates as an  $n = 1$  process with a pK of 6.35; a variation of  $\pm 0.15$  was found in different preparations. At low pH values (~6), the complex exhibits a clear band at 630 nm, usually assigned to high-spin heme with histidine and water occupying the fifth and sixth coordination sites, respectively. At high pH values, this band is bleached and the spectrum conforms to a low-spin form of ferric cyt *c*. The nature of the sixth ligand has been assigned by MCD spectroscopy, and it is reported that at this pH the ferric form of the CL complex comprises a mixed population with either a lysine residue (majority) or hydroxyl (minority) acting as the sixth ligand. This assignment is consistent with the fact that a number of ferric Met80 mutants of cyt *c* coordinate lysine at high pH.<sup>22</sup> The spectrum of the NO adduct was found to be independent of pH in the range of 6.5–7.5 where the photolysis experiments were performed.

**NO Binding Kinetics. Stopped-Flow Spectrophotometry.** When NO is mixed with the ferric cyt *c*/CL complex, the formation of the NO adduct could be observed to occupy the first ~0.5 s after mixing (Figure 2). The spectral transition (Figure 2) accompanying this process conformed well to that expected from examination of the static spectrum seen in Figure 1A. Figure 2 also illustrates a comparison of the



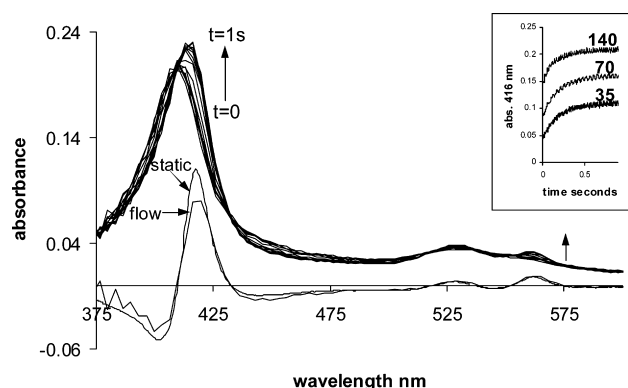
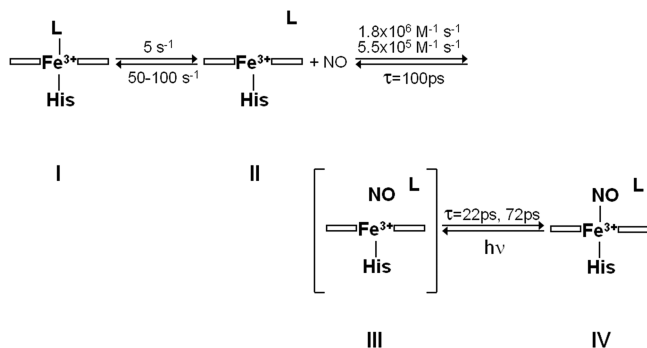


**Figure 2.** Reaction between the horse heart cyt *c*/CL complex and NO. Spectra were collected using a stopped-flow spectrometer. Spectra are shown at 0.002, 0.010, 0.020, 0.030, 0.050, 0.10, 0.20, 0.30, 0.40, 0.50, 0.60, 0.70, 0.80, 0.90, and 1.0 s. A comparison of the difference spectra (ferric/CL–NO minus ferric/CL) obtained statically (Figure 1) and kinetically ( $t = 1$  s minus  $t = 0.002$  s) is also given (the kinetic spectrum has been multiplied by 2 to account for the dilution in the stopped-flow experiment). The inset shows time courses for the combination of the NO–ferric cyt *c*/CL complex monitored at 416 nm and at three NO concentrations (35, 70, and 140  $\mu$ M). The three curves are offset for the sake of clarity. Other conditions: 2  $\mu$ M cyt *c* (after mixing), 20 mM sodium Hepes, 22  $^{\circ}$ C.

difference spectra calculated from the static and kinetic measurement. It can be seen that apart from differences due to the poorer resolution and larger bandwidth of the stopped-flow spectrophotometer there is good correspondence between the kinetic and static spectra indicating the absence of any faster process that had been lost in the dead time of the instrument. The time course could be fit adequately to a single exponential, the rate constant for which was independent of NO concentration and had a value of  $\sim 5$   $s^{-1}$ . This independence from NO concentration is illustrated in the inset of Figure 2, where the time course for NO binding is shown at three NO concentrations.

This result is consistent with a model (see Scheme 1) in which the rate of binding of NO to the heme is limited by the

#### Scheme 1



dissociation rate of the intrinsic ligand (predominantly lysine) from coordination to the heme, which is itself consistent with the pH titration curve given in Figure 1 that shows that at pH 7.5 the protein is >90% low-spin.

**Nanosecond Flash Photolysis.** When the NO adduct of the ferric cyt *c*/CL complex is exposed to nanosecond flash illumination, NO dissociated from the heme and a fraction of this was released into the bulk phase. Following illumination,

NO recombined with the heme in the dark to re-form the NO adduct. The time resolution of this method (nanosecond upward) is such that geminate recombination cannot be observed but only recombination from the bulk phase may be followed. Figure 3 shows the spectral distribution that

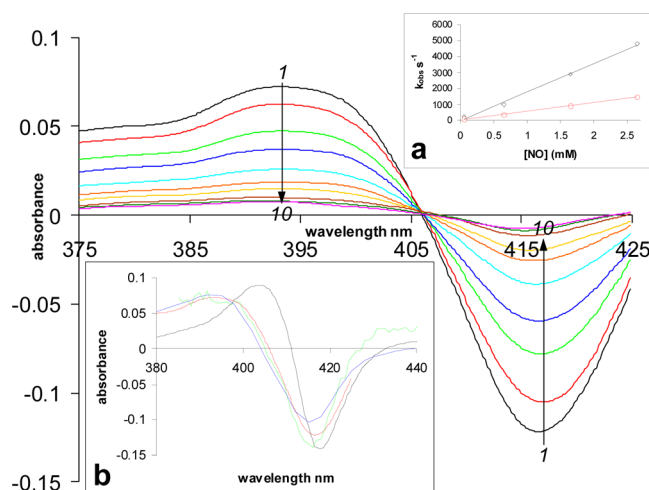


**Figure 3.** Nanosecond flash photolysis of the horse heart ferric cyt *c*/CL–NO complex. Difference spectra (1–10) at selected times (48, 96, 192, 288, 480, 720, and 960  $\mu$ s) following photolysis of NO from the cyt *c*/CL complex are shown. The difference spectra were constructed from the point by point accumulation of data at wavelengths of 375–425 nm every 5 nm. Inset a shows the rate constants of the fast (black) and slow (red) phase of NO rebinding as a function of NO concentration, monitored at 417 nm. Inset b shows a comparison of difference spectra (ferric cyt *c*/CL minus ferric cyt *c*/CL–NO) obtained statically (Figure 1) or from the laser photolysis experiments. The static difference spectrum (black line), the residual difference spectrum (green line), normalized, taken at 4 ns from the ultrafast experiment (see also the text and Figure 4). The difference spectra collected from the nanosecond laser experiments at low (10  $\mu$ M) and high (2 mM) NO concentrations are shown as blue and red lines, respectively. Conditions:  $\sim 5$   $\mu$ M cyt *c*, 20 mM Hepes (pH 7.4), 22  $^{\circ}$ C.

accompanies NO recombination. This figure presents the difference spectra (between the sample immediately after the flash and the final NO adduct, baseline) collected at a number of time points after laser photolysis. The spectra display a clear isosbestic point (405.5 nm) indicative of a single spectral transition. The initial spectrum (time zero) is compared in the inset of Figure 3 with the difference spectrum (ferric minus ferric–NO) obtained from the static spectra given in Figure 1A. It is apparent that the spectrum obtained after photolysis, at both high and low NO concentrations, and that obtained statically are very different. This is best explained by the proposition that NO displaces the intrinsic ligand, in agreement with the stopped-flow data, and that following photolysis this intrinsic ligand does not rebind before the NO has recombined to form the nitrosyl adduct. This is consistent with the observation that NO binding, unlike that seen in the stopped-flow experiments, is very rapid and dependent on NO concentration (see the time courses given as an inset of Figure 3). Analysis of the time courses for NO recombination showed these could be fit as the sum of two exponentials, the rate constant of each being linearly dependent on NO concentration yielding second-order rate constants for NO binding of  $1.8 \times 10^6$  and  $5.5 \times 10^5$   $M^{-1} s^{-1}$  (see the inset of Figure 3).



**Geminate NO Rebinding to the Ferric Cyt *c*/CL Complex.** On the femtosecond time scale, excitation of the ferric NO-bound cyt *c*/CL complex results in a bleaching of the ground state Soret band at 416 nm and an increased absorption at  $\sim 390$  nm, as expected for a five-coordinate ferric heme species<sup>23</sup> (Figure 4). Besides a very fast component ( $\sim 200$  fs), assigned to excited state photophysics of the heme,<sup>17,24</sup> global analysis of the data reveals a 22 ps component and a 72 ps component. The similarity of the DAS spectra of the 22 and 72 ps phases suggests that they reflect the same process, namely NO recombination but from two distinct conformations of the heme environment. The faster component (22 ps) comprises 49% of the amplitude associated with rebinding and the slower component (72 ps) 28%. The remainder, 23%, does not rebind within 4 ns, as indicated after the kinetic trace had been fit at 416 nm. The spectrum of this residual component is also compared with the difference spectrum obtained from the nanosecond laser photolysis, and the two are shown to be identical (Figure 3). This time course is compared in Figure 4B with that seen using either the NO–cyt *c* adduct or this in the presence of 5% EtOH. In both cases, all NO rebinding is geminate, with no NO escaping to the bulk phase. The EtOH did have an effect on the time course but leaves the caging effect of the heme pocket unchanged such that NO exit is not permitted. This demonstrates that while low concentrations of ethanol, necessary for the preparation of the complex (see Materials and Methods), affect the kinetics of the geminate recombination it is the CL that is responsible for allowing escape from the heme pocket.

## DISCUSSION

### Dynamics of Nitric Oxide within the Heme Pocket.

Nitric oxide has a high intrinsic affinity for the heme iron. In many heme proteins, NO is known to rebind on the picosecond time scale and in a multiphasic way that is very sensitive to the structure of the heme pocket.<sup>15</sup> The NO geminate recombination in the ferric state of the cyt *c*/CL complex is biphasic (22 and 72 ps phases) with a significant contribution of the asymptotic phase (23%), suggesting that dynamic processes of NO transitions are taking place between cavities and that a significant amount of NO escapes the heme pocket. Similar NO rebinding kinetics [13 ps (69%) and 63 ps (29%)] have been observed in the ferric AXCP–NO complex, but in this protein, hardly any NO escapes from the heme pocket.<sup>21</sup> In the absence of CL, the ferric cyt *c*–NO adduct rebinds in a monophasic way (time constant of 9.4 ps) to the heme iron and also a negligible amount of NO escapes from the heme pocket (3%).<sup>21</sup> However, substantial NO escape after photodissociation from ferric heme is not unprecedented, as  $\sim 30\%$  escape was reported from the ferric *b*-type heme-containing fraction of the NO complex of bacterial NO reductase.<sup>25</sup> The open nature of the ferric cyt *c*/CL complex that we find is consistent with the structural studies of this complex using fluorescently labeled variants of horse cyt *c*.<sup>26</sup> These studies demonstrated an extensive unfolding of a section of the cyt *c* molecule driven largely by electrostatic interactions between the protein and CL. A model provided in this study suggested much more open access to the heme group in the complex.

Interestingly, a significant amount of NO escapes the heme pocket and does not rebind on an early time scale in both redox states of the cyt *c*/CL complex (11% NO escape in the reduced cyt *c*/CL complex, 23% NO escape in the oxidized cyt *c*/CL

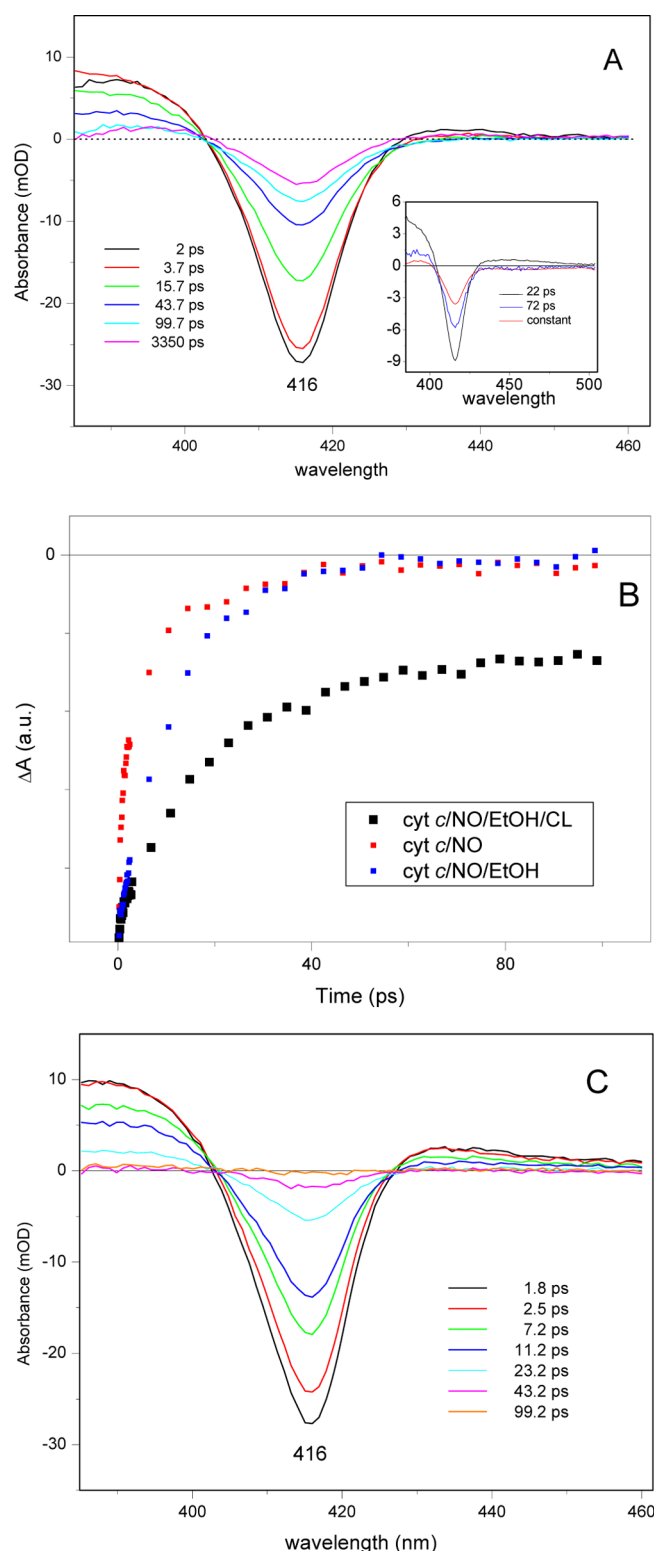


**Figure 4.** Ultrafast spectroscopy of the ferric cyt *c*/CL–NO adduct. (A) Transient absorption spectra of the oxidized cyt *c*/CL–NO complex at different delay times in the pico- to nanosecond time range. The inset shows the analysis in terms of decay-associated spectra, i.e., spectra associated with the time constants ( $\tau = 1/k$ ) given in the figure. (B) Kinetics at 416 nm of the cyt *c*/CL–NO complex, the cyt *c*–NO complex, and the cyt *c*/EtOH–NO complex. (C) Transient absorption spectra of the NO-bound cyt *c*/EtOH complex.



complex<sup>12</sup>). In contrast, in the CL-free cyt *c*, hardly any NO escapes from the heme pocket (see above). This implies the presence of a ligand exchange pathway that facilitates NO release in the CL-bound form. Given the different NO escape ratios in the reduced and oxidized cyt *c*/CL complexes, it might be suggested that the oxidation state of cyt *c* affects the binding of CL, and as a result, the conformational changes induced in cyt *c* by CL binding are slightly different. Alternatively, however, as NO has a higher affinity for ferrous heme than ferric heme,<sup>27</sup> this may be reflected in faster NO rebinding in the reduced complex (7 ps<sup>12</sup>) than in the oxidized one (22 and 72 ps) and thus a smaller effective escape yield. Whereas the biphasicity of the rebinding kinetics complicates the assessment of a complete reaction scheme, the ensemble of rate constants and amplitudes of the picosecond phases indicate that the intrinsic time constant for the escape of NO from the heme pocket in the ferric complex is ~100 ps.

The simplest, but not sole, explanation for the large escape fraction from the ferric form is, therefore, that as the geminate rebinding process is slower in the ferric species, this allows escape from the heme pocket to compete more efficiently with rebinding. We cannot at present exclude the alternative explanation, namely, that the structure of the pocket is more open in the ferric cyt *c*/CL complex than in the ferrous species.

**Dynamics of Entry of NO into the Heme Pocket.** The static spectra taken with the titration data (Figure 1) suggest that at pH 7.5 the bulk of the ferric protein in the CL complex is low-spin with an intrinsic ligand occupying the sixth coordination site of the iron *trans* to a histidine ligand. We and others have shown that in this complex the 695 nm band, indicative of methionine ligation and present in the native protein, is bleached.<sup>10,12,28</sup> The intrinsic ligand cannot therefore be the native methionine but in keeping with recent MCD studies is likely to be a lysine residue (cf. carboxy methyl cyt *c*, some Met80X mutants of cyt *c*, the alkaline form of native cyt *c* and cyt *f*<sup>22,29,30</sup>). These data demonstrate therefore that CL displaces methionine from coordinating to the iron and at pH 7.5 also causes this to be replaced (largely) by a lysine. This proposal is also consistent with the stopped-flow data that show that the complex binds NO in a single process that is independent of NO concentration and rate-limited at ~5 s<sup>-1</sup>, a rate constant we assign to the dissociation rate constant of the putative lysine ligand.

Photolysis experiments, monitoring NO recombination from the bulk phase, show that this process is fast and dependent on NO concentration in the range of 100  $\mu$ M to 3 mM, indicating that under these conditions NO binding is not limited by the requirement to replace an existing ligand. This interpretation is supported by the difference spectrum that is clearly different from that obtained statically yet identical to the final spectrum obtained from the ultrafast laser photolysis experiments. This is expected if NO rebinds to five-coordinate heme species following photolysis but replaces a ligand in the stopped-flow and static experiments such that the heme remains six-coordinate throughout the experiment.

Even at the lowest NO concentration used to generate the difference spectrum (10  $\mu$ M), there was no evidence of competition with the intrinsic ligand, as shown by the invariance of the spectra with respect to NO concentration (see Figure 3), implying that binding of this ligand must take place with a rate constant of <100 s<sup>-1</sup>.

**Model for NO Binding.** The data presented above may be summarized in Scheme 1. At pH 7.5, the ferric complex exists

as a low-spin hexacoordinate species (I) with lysine as the predominate ligand (L). In the stopped-flow experiments, NO can bind to the iron only once species II is populated. This occurs with a rate constant (~5 s<sup>-1</sup>) given by the dissociation of the ligand (L), hence the observed NO concentration-independent time courses. The rate constant for binding of L to the ferric iron must, by examination of the titration curve that indicates that the ferric form is >90% in the low-spin form, be ~50–100 s<sup>-1</sup>. The photolysis data were collected starting with the NO-bound derivative (IV). On photolysis of NO from the heme, it moves into the internal cavity of the heme pocket (depicted as species III). From this location, a fraction of the NO escapes the heme pocket (23%) with a rate constant of ~100 ps<sup>-1</sup>. The nanosecond laser experiments monitor the recombination of NO from the bulk solution to the pentacoordinate complex (II). The recombination kinetics show that there are two species present differing in rate constant. However, the spectrum associated with binding of NO to each is identical as shown by the isosbestic points in the difference spectra.

The ultrafast photolysis experiments monitor the geminate recombination of NO with species III to re-form the nitrosyl adduct (IV).

**Implications for the Cyt *c*-Mediated Apoptotic Pathway.** When, in the context of apoptosis in the living cell, one considers the mechanisms we have presented above, it is proper to ask how appropriate the model is that we have used to mimic the inner mitochondrial membrane. First, the membrane fragments that we have used are comprised entirely of CL, and this is certainly not the composition of the mitochondrial membrane. However, this criticism of the system may not be as severe as it seems. In this regard, we may note that mixed phospholipid liposomes that contain only some 25% CL interact with cyt *c* and lead to the transformation in the protein involving displacement of Met80 from the heme.<sup>10</sup> Without CL in the liposome, this does not occur. Thus, the conformational and functional changes caused by CL occur when it is present in membranes as a minor component, and thus, these are not a consequence of the action of pure CL only. It is reasonable to presume therefore that in the mitochondrion, where CL amounts to ~20% in the inner membrane, the CL may act to transform a fraction of bound cyt *c* as described.

The potential involvement of NO in the regulation of programmed cell death has already been suggested because of its increased production in the early stages of apoptosis.<sup>31</sup> NO seems to affect apoptosis in a complex way that may be either stimulatory or inhibitory.<sup>32</sup> Our previous work on the interaction of NO with the reduced cyt *c*/CL complex has demonstrated the remarkable influence CL exerts on the ligand binding properties of cyt *c*, promoting conformational changes in the protein that facilitate NO binding and lead to dissociation of the proximal histidine residue on NO binding.<sup>12</sup> In agreement with our previous studies,<sup>10,12</sup> the work presented here also reveals the formation of a ligand exchange pathway in the cyt *c*/CL complex. This more open access to the heme is expected to facilitate the reaction with H<sub>2</sub>O<sub>2</sub> and thus allow the peroxidase activity of the complex.<sup>33,34</sup> However, unlike in the reduced cyt *c*/CL complex, NO does not appear to bind at the proximal site of the oxidized complex.<sup>12</sup> Recent studies have pointed toward a strong inhibitory effect of NO on the peroxidase activity of the cyt *c*/CL complex.<sup>20</sup> Although distal site binding of NO at the cyt *c*/CL complex seems to favor such an inhibitory effect, the formation of the Fe–NO complex has



been considered a rather unimportant mechanism of NO regulation of the peroxidatic activity of the cyt *c*/CL complex.<sup>20</sup> The formation of stable Fe–NO complexes suggests that the oxidized cyt *c*/CL complex may help to increase the resistance of mitochondria to NO toxicity. Furthermore, the oxidized cyt *c*/CL complex may act as a complex that traps NO and subsequently, under reducing conditions, can contribute to a controlled NO release in mitochondria during the early stages of apoptosis, as previously proposed for the reduced cyt *c*/CL complex.<sup>12</sup>

## AUTHOR INFORMATION

### Corresponding Author

\*E-mail: silkgi@essex.ac.uk. Telephone: +44 01206 873015.

### Funding

S.M.K. was the recipient of a grant from the Région Ile-de-France and M.T.W. from the Royal Society UK.

### Notes

The authors declare no competing financial interest.

## REFERENCES

- (1) Iverson, S. L., and Orrenius, S. (2004) The cardiolipin-cytochrome *c* interaction and the mitochondrial regulation of apoptosis. *Arch. Biochem. Biophys.* 423, 37–46.
- (2) Basova, L. V., Kurnikov, I. V., Wang, L., Ritov, V. B., Belikova, N. A., Vlasova, I. I., Pacheco, A. A., Winnica, D. E., Peterson, J., Bayir, H., Waldeck, D. H., and Kagan, V. E. (2007) Cardiolipin Switch in Mitochondria: Shutting off the Reduction of Cytochrome *c* and Turning on the Peroxidase Activity. *Biochemistry* 46, 3423–3434.
- (3) Kagan, V. E., Bayir, H. A., Belikova, N. A., Kapralov, O., Tyurin, Y. Y., Tyurin, V. A., Jiang, J., Stoyanovsky, D. A., Wipf, P., Kochanek, P. M., Greenberger, J. S., Pitt, B., Shvedova, A. A., and Borisenko, G. (2009) Cytochrome *c*/cardiolipin relations in mitochondria: A kiss of death. *Free Radical Biol. Med.* 46, 1439–1453.
- (4) Twiddy, D., Brown, D. G., Adrain, C., Jukes, R., Martin, S. J., Cohen, G. M., MacFarlane, M., and Cain, K. (2004) Proapoptotic-proteins released from the mitochondria regulate the protein composition and caspase-processing activity of the native Apaf1/caspase-9 apoptosome complex. *J. Biol. Chem.* 279, 19665–19682.
- (5) Martin, M. C., Allan, L. A., Lickrish, M., Sampson, C., Morrice, N., and Clarke, P. R. (2005) Protein Kinase A Regulates Caspase-9 Activation by Apaf-1 Downstream of Cytochrome *c*. *J. Biol. Chem.* 280, 15449–15455.
- (6) Hancock, J. T., Desikan, R., and Neill, S. J. (2001) Does the redox status of cytochrome *c* act as a fail-safe mechanism in the regulation of programmed cell death? *Free Radical Biol. Med.* 31, 697–703.
- (7) Brown, G. C., and Borutaite, V. (2008) Regulation of apoptosis by the redox state of cytochrome *c*. *Biochim. Biophys. Acta* 1777, 877–881.
- (8) Chung, H. T., Pae, H. O., Choi, B. M., Billiar, T. R., and Kim, Y. M. (2001) Nitric oxide as a bioregulator of apoptosis. *Biochem. Biophys. Res. Commun.* 282, 1075–1079.
- (9) Bilban, M., Haschemi, A., Wegiel, B., Chin, B. Y., Wagner, O., and Otterbein, L. E. (2008) Heme oxygenase and carbon monoxide initiate homeostatic signaling. *J. Mol. Med.* 86, 267–279.
- (10) Kapetanaki, S. M., Silkstone, G., Husu, I., Liebl, U., Wilson, M. T., and Vos, M. H. (2009) Interaction of Carbon Monoxide with the Apoptosis-Inducing Cytochrome *c*-Cardiolipin Complex. *Biochemistry* 48, 1613–1619.
- (11) Lawson, D. M., Stevenson, C. E. M., Andrew, C. R., and Eady, R. R. (2000) Unprecedented proximal binding of nitric oxide to heme: Implications for guanylate cyclase. *EMBO J.* 19, S661–S671.
- (12) Silkstone, G., Kapetanaki, S. M., Husu, I., Vos, M. H., and Wilson, M. T. (2010) Nitric Oxide Binds to the Proximal Heme Coordination Site of the Ferrocycytochrome *c*/Cardiolipin Complex:

Formation Mechanism and Dynamics. *J. Biol. Chem.* 285, 19785–19792.

- (13) Stone, J. R., and Marletta, M. A. (1994) Soluble Guanylate Cyclase from Bovine Lung: Activation with Nitric Oxide and Carbon Monoxide and Spectral Characterization of the Ferrous and Ferric States. *Biochemistry* 33, 5636–5640.
- (14) Yoshimura, T., Suzuki, S., Nakahara, A., Iwasaki, H., Masuko, M., and Matsubara, T. (1986) Spectral Properties of Nitric-Oxide Complexes of Cytochrome-*c*' from *Alcaligenes* sp. Ncib 11015. *Biochemistry* 25, 2436–2442.
- (15) Vos, M. H. (2008) Ultrafast dynamics of ligands within heme proteins. *Biochim. Biophys. Acta* 1777, 15–31.
- (16) Dupre, S., Brunori, M., Wilson, M. T., and Greenwood, C. (1974) Kinetics of Carbon-Monoxide Binding and Electron-Transfer by Cytochrome-*c* Polymers. *Biochem. J.* 141, 299–304.
- (17) Martin, J.-L., and Vos, M. H. (1994) Femtosecond spectroscopy of ligand rebinding in heme proteins. *Methods Enzymol.* 232, 416–430.
- (18) Liebl, U., Lambry, J.-C., Leibl, W., Breton, J., Martin, J.-L., and Vos, M. H. (1996) Energy and electron transfer upon selective femtosecond excitation of pigments in membranes of *Helicobacter mobilis*. *Biochemistry* 35, 9925–9934.
- (19) Yoshimura, T., and Suzuki, S. (1988) The pH-Dependence of the Stereochemistry around the Heme Group in No Cytochrome-C (Horse Heart). *Inorg. Chim. Acta* 152, 241–249.
- (20) Vlasova, I. I., Tyurin, V. A., Kapralov, A. A., Kurnikov, I. V., Osipov, A. N., Potapovich, M. V., Stoyanovsky, D. A., and Kagan, V. E. (2006) Nitric Oxide Inhibits Peroxidase Activity of Cytochrome *c*. Cardiolipin Complex and Blocks Cardiolipin Oxidation. *J. Biol. Chem.* 281, 14554–14562.
- (21) Cianetti, S. M. (2005) Ph.D. Thesis, University of Florence and University of Paris 6.
- (22) Silkstone, G., Stanway, G., Brzezinski, P., and Wilson, M. T. (2002) Production and characterisation of Met80X mutants of yeast iso-1-cytochrome *c*: Spectral, photochemical and binding studies on the ferrous derivatives. *Biophys. Chem.* 98, 65–77.
- (23) Petrich, J. W., Poyart, C., and Martin, J.-L. (1988) Photophysics and reactivity of heme proteins: A femtosecond absorption study of hemoglobin, myoglobin and protoheme. *Biochemistry* 27, 4049–4060.
- (24) Franzen, S., Kiger, L., Poyart, C., and Martin, J. L. (2001) Heme photolysis occurs by ultrafast excited state metal-to-ring charge transfer. *Biophys. J.* 80, 2372–2385.
- (25) Kapetanaki, S. M., Field, S. J., Hughes, R. J. L., Watmough, N. J., Liebl, U., and Vos, M. H. (2008) Ultrafast ligand binding dynamics in the active site of native bacterial nitric oxide reductase. *Biochim. Biophys. Acta* 1777, 919–924.
- (26) Hanske, J., Toffey, J. R., Morenz, A. M., Bonilla, J., Schiavoni, H., and Pletneva, E. V. (2012) Conformational properties of cardiolipin-bound cytochrome *c*. *Proc. Natl. Acad. Sci. U.S.A.* 109, 125–130.
- (27) Hoshino, M., Ozawa, K., Seki, H., and Ford, P. C. (1993) Photochemistry of nitric oxide adducts of water-soluble iron(III) porphyrin and ferrihemoproteins studied by nanosecond laser photolysis. *J. Am. Chem. Soc.* 115, 9568–9575.
- (28) Vladimirov, Y. A., Proskurnina, E. V., Izmailov, D. Y., Novikov, A. A., Brusnichkin, A. V., Osipov, A. N., and Kagan, V. E. (2006) Mechanism of activation of cytochrome *c* peroxidase activity by cardiolipin. *Biochemistry (Moscow, Russ. Fed.)* 71, 989–997.
- (29) Bradley, J. M., Silkstone, G., Wilson, M. T., Cheesman, M. R., and Butt, J. N. (2011) Probing a complex of cytochrome *c* and cardiolipin by magnetic circular dichroism spectroscopy: Implications for the initial events in apoptosis. *J. Am. Chem. Soc.* 133, 19676–19679.
- (30) Davis, D. J., Frame, M. K., and Johnson, D. A. (1988) Resonance Raman spectroscopy indicates a lysine as the sixth iron ligand in cytochrome *f*. *Biochim. Biophys. Acta* 936, 61–66.
- (31) Schonhoff, C. M., Gaston, B., and Mannick, J. B. (2003) Nitrosylation of Cytochrome *c* during Apoptosis. *J. Biol. Chem.* 278, 18265–18270.
- (32) Chung, H. T., Pae, H. O., Choi, B. M., Billiar, T. R., and Kim, Y. M. (2001) Nitric oxide as a bioregulator of apoptosis. *Biochem. Biophys. Res. Commun.* 282, 1075–1079.



(33) Vladimirov, Y. A., Proskurnina, E. V., Izmailov, D. Y., Novikov, A. A., Brusnichkin, A. V., Osipov, A. N., and Kagan, V. E. (2006) Cardiolipin activates cytochrome *c* peroxidase activity since it facilitates H<sub>2</sub>O<sub>2</sub> access to heme. *Biochemistry (Moscow, Russ. Fed.)* 71, 998–1005.

(34) Kapralov, A. A., Kurnikov, I. V., Vlasova, I. I., Belikova, N. A., Tyurin, V. A., Basova, L. V., Zhao, Q., Tyurina, Y. Y., Jiang, J., Bayir, H., Vladimirov, Y. A., and Kagan, V. E. (2007) The hierarchy of structural transitions induced in cytochrome *c* by anionic phospholipids determines its peroxidase activation and selective peroxidation during apoptosis in cells. *Biochemistry* 46, 14232–14244.